

ELM mitigation by externally induced ELMs - Physics and Prospects

P.T.Lang*, J.Bucalossi¹, L.Fattorini², K.Gal³, J.Hobirk, L.D.Horton, A.Kallenbach,
J.Lister⁴, S.Kalvin³, G.Kocsis³, M.E.Manso², M.Maraschek, Y.Martin⁴, V.Mertens,
R.Neu, J.Neuhauser, T.Pütterich, W.Schneider, A.C.C.Sips, W.Suttrop, G.Veress³,
ASDEX Upgrade Team

*Max-Planck-Institut für Plasmaphysik, EURATOM Association,
Boltzmannstr. 2, 85748 Garching, Germany*

¹ *CEA Cadarache, 13108 St Paul-Lez-Durance Cedex, France,*

² *Centro de Fusão Nuclear, IST, 1049-001 Lisboa, Portugal*

³ *KFKI-RMKI, EURATOM Association, P.O. Box 49, H-1525 Budapest-114, Hungary*

⁴ *CRPP-EPFL, CH-1015 Lausanne, Switzerland,*

* *Corresponding author; e-mail: peter.lang@ipp.mpg.de*

1. Introduction

In ITER the ELM induced power load is a main area of concern for the type-I ELMy H-mode [1]. ELM control and mitigation aims on a modification of the ELM frequency f_{ELM} causing a reduction of the ELM energy ΔW_{ELM} [2]. In JET and ASDEX Upgrade for plasmas with a ratio of total and thermal energy content ~ 1 a relation $f_{ELM} \times \Delta W_{ELM} = 0.2 \times P_{loss}$ was found (P_{loss} : power lost to divertor) [3]. Various methods are currently under investigation usually targeting the ELM drive terms edge pressure gradient p'_{edge} and current j_{edge} in the steep gradient zone of the transport barrier at the plasma edge. One technique is the injection of cryogenic Deuterium (D) pellets [4], imposing strong local 3D perturbations. Magnetic triggering, relying on the edge current induction caused by a vertical motion of the plasma column in an up-down asymmetric magnetic field configuration [5], aims on altering profiles over the entire toroidal circumference. For both techniques a relation for the plasma energy was found significantly less than $W \sim f_{ELM}^{-0.6}$ observed for constant heating power in the case of intrinsic ELMs [3]. Beyond these two techniques successfully applied at ASDEX Upgrade, further approaches had been tested or are currently under investigation. Information derived from different approaches are expected to broaden the application potential, give insight in the underlying physics of ELMs and ELM control enabling in turn for further optimisation of the techniques. Results can be obtained even if a method fails to trigger prompt ELMs as in case of a supersonic D gas jet.

2. Experimental set-up

We used a lower single null (LSN) configuration with $I_P = 1MA$, $B_t = -2.7T$, $q_{95} = 4.9$, $\kappa = 1.6$, $\delta^u = 0.12$ and $\delta^l = 0.37$. Stable and robust operation in the type-I ELM regime with a low natural ELM frequency $f_{ELM}^0 \sim 25 - 45Hz$ was achieved by keeping the auxiliary heating close above the L-H transition power threshold. Typically, 5 MW of NBI and 1- 2 MW central ICRH (preventing impurity accumulation) was applied. In this scenario both investigation of ELM mitigation applying driving frequencies up to 80 Hz as well as perturbative ELM triggering (2 - 6 Hz) was performed. Four different techniques were applied in this study so far: injection of D pellets, laser blow off (LBO) of micropellets, magnetic triggering and supersonic molecular D gas jet injection. Pellets are launched from the magnetic high field side (HFS). Available velocities v_P range from 240 to 1000 m/s, masses m_P from 2 to 35×10^{19} D-atoms. A Supersonic Pulsed Gas Injector was used delivering a molecular D jet (speed 1.8 km/s) from the low field side

(LFS) containing $1 - 5 \times 10^{19} D_2$. The plasma movement required for magnetic triggering was performed by the poloidal magnetic field coils controlled by the plasma position and shape control system. The system allows feed forward control of the plasma contour with a cycle time of 2.5 ms and motional amplitudes of up to about 6 cm at an absolute precision of about 0.5 cm. LBO from the LFS was done at up to 20 Hz. Two different target types were used: carbon (C) spheres ($r = 100\mu m$) glued on a glass surface and etched aluminium (Al) on quartz targets ($10\mu m$ thick disk with $r = 50\mu m$) [6].

3. Results

3.1. Global impact and operational features

For D pellet injection a relation of $W \sim f_{ELM}^{-0.16}$ was achieved, $W \sim f_{ELM}^{-0.22 \pm 0.06}$ was found for magnetic triggering. It is still unclear if these virtually identical values are caused by a common reason or by chance due to different processes immanent to the method as e.g. additional convection losses imposed by the pellet fuelling. As in any case the relation found is superior to the intrinsic ELM scaling, the proof-of-principle for successful and beneficial ELM control was obtained. Obviously, ELM controlling can be achieved by imposing different physics approaches while the essential operational features are of general rather than method related nature.

For the D pellets it was found that any pellet injected during type-I ELMy H-mode phases triggered a prompt ELM. This release is attributed to a strong localised 3D perturbation resulting in the onset of the ELM instability on the sub-ms time scale once the pellet hits the region within the gradient zone. In case of magnetic triggering the effect is related to the induced edge current profile, which gradually changes during the motion. Once steady state is achieved and provided sufficient vertical motion is imposed (approx. 5 mm, about the same value as caused by intrinsic ELMs), one ELM is released per motion cycle. Although ELMs occur preferentially when the plasma achieves its maximum downward velocity, there is still some statistics in the triggering probability within an ELM cycle. In order to conduct experiments investigating the ELM triggering we concentrated on the D pellet tool. It is more easy to apply, raises no vessel resonance risk potential, allows for more precision in the temporal and spatial diagnosing and its global impact can be neglected in case of low pellet rates. Furthermore, pellets create stronger perturbations than magnetic triggering as demonstrated in the combination experiment shown in figure 1. Here, magnetic triggering was applied at a frequency of 55.6 Hz and pellet triggering at 62.5 Hz. Due to the timing applied, pellets were "sampling" the motion cycle at 2ms at a total period time of 144ms (shaded area). Clearly pellets form the dominant trigger perturbation while the combined ELM frequency $f_{comb} = 73.9 Hz$ exceeds both single driver frequencies. Still, every pellet triggers an ELM irrespective of the current phase determined by the vertical motion, even in cases where the vertical motion yields a maximum stabilisation for the ELM. In contrast, magnetic triggering only achieves ELM release in phases where its maximum destabilisation occurs between two pellet triggered ELMs. No magnetic ELM trigger is detected in the vicinity of a pellet triggered ELM. For the supersonic gas jet injection the resulting perturbation was found insufficient for prompt ELM triggering. An impact on the ELM cycle can be obtained due to particle fuelling but only on a ms-time scale. For the LBO approach so far no significant correlation between C or Al pellet injection and the ELM behaviour was detected.

3.2. Local impact and ELM dynamic features

The basic observation made comparing triggered ELMs to their intrinsic counterparts was they are virtually identical at the same f_{ELM} values [7]. In case of pellet injection

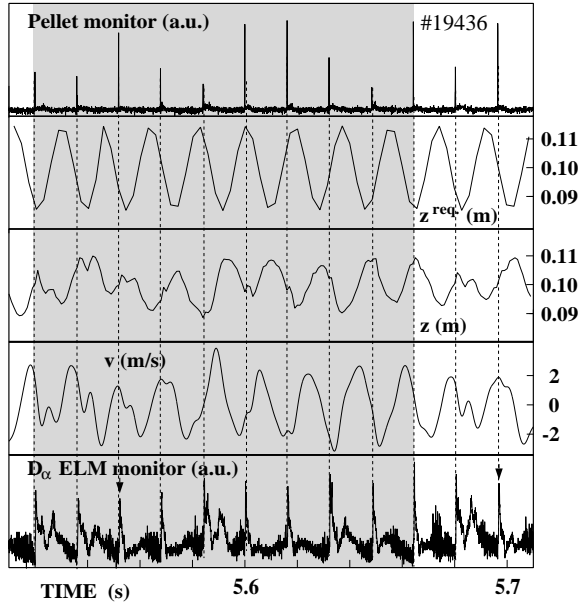


Figure 1: Combination of pellet and magnetic ELM triggering, pellets probing the vertical motion cycle.

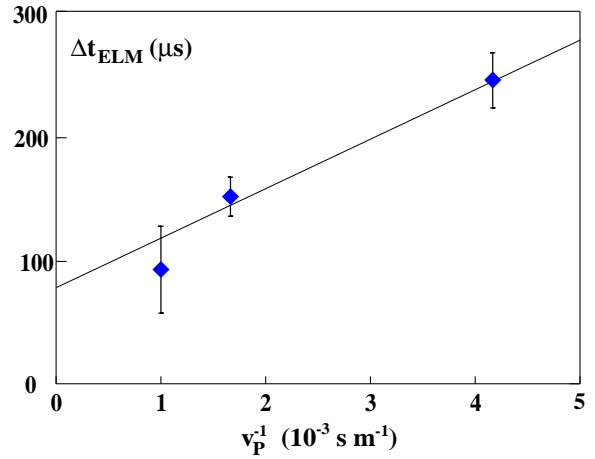


Figure 2: Delay of ELM onset to pellet crossing the separatrix versus inverse pellet velocity. Data indicate for an intrinsic ELM onset time of $\sim 80\mu\text{s}$, the ELM trigger seed perturbation is generated $\sim 40\text{mm}$ inside the separatrix along the pellet path.

this applies only for the smallest pellets. Larger pellets cause longer ELMs (expelling more particles) or even trigger an ELM cascade. However, triggered ELMs can break the relation between f_{ELM} and edge plasma parameters like the collisionality ν^* [8]. Thus, mitigation is based on the fact that ELMs can be driven at frequencies different from the intrinsic value related to the plasma parameters but at a size adapted to the driving frequency.

Knowing precisely timing and strengths of the perturbations imposed by D pellets and the gas jets, investigations on the ELM triggering process were performed. The major question in this context was where the seed perturbation for the ELM is localised. Some information is already provided by the fact that pellets can trigger prompt ELMs while the gas jet fails to do so. Obviously, different perturbation patterns are bordering the required trigger threshold. The origin of the ELM trigger is thought to be formed by the local 3D particle deposition. This perturbation spreads out quickly along field lines. The ELM trigger is not necessarily due to the direct impact but can also result from the spreading perturbation with some time delay. From its onset, the ELM grows until it becomes detectable. Hence, the detected ELM onset is delayed by t_{os} with respect to its activating perturbation imposed.

For the gas jet it has been found [9] that significant particle deposition takes place only close to and outside the separatrix due to self blocking of the beam. Pellets penetrate deep into the plasma far beyond the pedestal region. Pellets trigger ELMs irrespective to their injection path as also LFS injection was found to trigger ELMs. A perturbation strength monitor is provided by the measured D_α ablation radiation proportional to the pellet particle ablation rate $\frac{dN}{dt}(t)$ [10]. Using information derived by a fast framing camera system on the pellet motion in the plasma or by comparing the measured $\frac{dN}{dt}(t)$ with modelling results it is possible to derive $\frac{dN}{dt}(\vec{r})$ (with $\vec{r}(t)$ the pellet position) [11]. For each pellet, the time delay Δt observed between passing a reference point \vec{r}_0 and the ELM onset is composed from t_{os} and the flight time to reach \vec{r}_t where the ELM trigger is

seeded. Possibly the pellet causes multiple ELM trigger seed perturbations, this way \vec{r}_t refers to the seed causing the first detected ELM component. Assuming the pellet moves with constant initial v_P along its designated path, $\Delta t_{ELM} = t_{os} + \frac{r_t - r_0}{v_P}$. Due to changes in $\frac{dN}{dt}(r)$, t_{os} and r_t can vary when m_P and v_P are altered. Also, observations of slightly curved pellet trajectories indicate changes of v_P . Such effects will be studied in more detail later on, but they seem to be of minor importance. The analysis presented here was performed for virtually identical plasma conditions assuming constant v_P , t_{os} and r_t . We believe a refined analysis will alter the data shown only within their error bars. Figure 2 shows Δt_{ELM} obtained for different v_P versus $1/v_P$ taking the separatrix crossing r_{sep} as reference. The analysis yields $t_{os} \sim 80\mu s$ and $r_t - r_{sep} \sim 40mm$. Mapped to the outer horizontal mid plane, the trigger seed position is approx. 13mm inside the separatrix close to the point the pressure profile is steepest. The observed ELM onset delay would be in accordance with ionic sound speed expansion of the pellet cloud finally triggering the ELM at the LFS in the region of unfavourable flux surface curvature. This result fits also well to the observation made by the gas jet approach. Even strong perturbations in the vicinity of the separatrix are insufficient for ELM triggering.

4. Prospects

It became already clear in ELM control experiments using D pellets that only a minor fraction of the injected particles are sufficient for ELM triggering. Taking into account t_{os} , this fraction turns out to be even smaller. Penetration to the centre of the pedestal is obviously sufficient. In the case of pellet injection this can be achieved using sizes virtually negligible with respect to fuelling. Hence, fuelling constraints are expected to vanish if appropriate pellets are injected. In the case that much smaller pellets are employed however it might become necessary to compensate for the reduction of ablation rate by a smaller v_P . Pellet injection systems optimised for ELM controlling should thus employ small and slow pellets - presumably from the LFS side. A system in line with these requirements is in development on AUG and expected to become operational at the end of 2005. Beyond its operational advantages, this system will also enhance the spatial resolution of the investigations due to the slower v_P .

Investigations so far already showed that there are ways to control ELMs in a very beneficial way, requirements to achieve ELM trigger can be fulfilled relatively simply. Further on, there is still headroom for optimisation of the tool by reducing unwanted side effects. Finally, it could be possible to apply techniques more easy to handle as magnetic triggering or cryogenic D pellets. One option would be the injection of room temperature solid pellets. Corresponding investigations are ongoing.

References

- [1] FEDERICI, F. et al., Plasma Phys. Controlled Fusion **45** (2003) 1523.
- [2] POLEVOI, A. et al., Nucl. Fusion **43** (2003) 1072.
- [3] HERRMANN, A., Plasma Phys. Controlled Fusion **44** (2002) 883.
- [4] LANG, P.T. et al., Nucl. Fusion **43** (2003) 1110.
- [5] DEGELING, A. et al., Plasma Phys. Controlled Fusion **45** (2003) 1637.
- [6] ZOLETNIK, S. et al., Rev. Sci. Instrum. **66** (1995) 2904.
- [7] LANG, P.T. et al., Nucl. Fusion **44** (2004) 665.
- [8] URANO, H. et al., Plasma Phys. Controlled Fusion **46** (2004) A315.
- [9] LANG, P.T. et al., Plasma Phys. Controlled Fusion **47** (2005) in press.
- [10] MC NEILL, D., J. Nucl. Mater. **162-164** (1989) 476.
- [11] KALVIN, S. et al., this conference (P2.078).